Monthly Notices
of the
ROYAL ASTRONOMICAL SOCIETY

Mon. Not. R. Astron. Soc. **401,** 2521–2530 (2010) doi:10.1111/j.1365-2966.2009.15827.x

Testing Newtonian gravity with AAOmega: mass-to-light profiles and metallicity calibrations from 47 Tuc and M55

Richard R. Lane,[1⋆] László L. Kiss,[1,2] Geraint F. Lewis,[1] Rodrigo A. Ibata,[3] Arnaud Siebert,[3] Timothy R. Bedding[1] and Péter Székely[4]

[1]*Sydney Institute for Astronomy, School of Physics, A29, University of Sydney, NSW, Australia 2006*
[2]*Konkoly Observatory of the Hungarian Academy of Sciences, PO Box 67, H-1525 Budapest, Hungary*
[3]*Observatoire Astronomique, Universite de Strasbourg, CNRS, 67000 Strasbourg, France*
[4]*Department of Experimental Physics, University of Szeged, Szeged 6720, Hungary*

Accepted 2009 October 4. Received 2009 October 2; in original form 2009 September 1

ABSTRACT

Globular clusters (GCs) are an important test bed for Newtonian gravity in the weak-acceleration regime, which is vital to our understanding of the nature of the gravitational interaction. Recent claims have been made that the velocity dispersion profiles of GCs flatten out at large radii, despite an apparent paucity of dark matter (DM) in such objects, indicating the need for a modification of gravitational theories. We continue our investigation of this claim, with the largest spectral samples ever obtained of 47 Tucanae (47 Tuc) and M55. Furthermore, this large sample allows for an accurate metallicity calibration based on the equivalent widths of the calcium triplet lines and *K*-band magnitude of the Tip of the Red Giant Branch. Assuming an isothermal distribution, the rotations of each cluster are also measured with both clusters exhibiting clear rotation signatures. The global velocity dispersions of NGC 121 and Kron 3, two GCs in the Small Magellanic Cloud, are also calculated. By applying a simple dynamical model to the velocity dispersion profiles of 47 Tuc and M55, we calculate their mass-to-light profiles, total masses and central velocity dispersions. We find no statistically significant flattening of the velocity dispersion at large radii for M55, and a marked *increase* in the profile of 47 Tuc for radii greater than approximately half the tidal radius. We interpret this increase as an evaporation signature, indicating that 47 Tuc is undergoing, or has undergone, core-collapse, but find no requirement for DM or a modification of gravitational theories in either cluster.

Key words: gravitation – stellar dynamics – globular clusters: individual.

1 INTRODUCTION

The nature of the gravitational interaction is one of the most important concepts in astrophysics, yet complete comprehension of this interaction is still elusive. The so-called Pioneer and Fly-by anomalies, where spacecrafts exhibit behaviour that is unexpected from Newtonian and general relativity gravitation theories, outline this lack of understanding (see Anderson et al. 2002; de Diego 2008, and references therein), although these examples may have more mundane explanations. More importantly, it has been claimed that several globular clusters (GCs; ω Centauri, M15, M30, M92 and M107) exhibit a flattening of their velocity dispersion profiles at radii $R \sim \frac{r_t}{2}$, where r_t is the tidal radius of the cluster (Scarpa, Marconi & Gilmozzi 2003, 2004a,b). The authors claim that either dark matter (DM) or a modification of gravitational theory is required to explain their results.

Modified theories of gravity (MOG; see Durrer & Maartens 2008, for a review of modified gravity theories) and those of Newtonian dynamics (MOND; Milgrom 1983) have been shown to solve some of the discrepancies. However, these are not universal theories and to-date have only been applied to specific instances (e.g. the Bullet Cluster and galaxy rotation curves; see Angus, Famaey & Zhao 2006; Sanders & Noordermeer 2007, respectively). MOG theories diverge from Newtonian gravity in the high-acceleration regime and MOND diverges from Newton in the low-acceleration regime. Therefore, if either of these theories were correct, the effect should be measurable at the predicted accelerations. Independent of MOG or MOND theories, testing the gravitational interaction at low accelerations is essential to the overall understanding of gravity.

GCs are an ideal testing ground for weak-field gravitation because the accelerations experienced by stars at large radii are below

⋆E-mail: rlane@physics.usyd.edu.au

the limit where DM, or a modified gravitation theory, is required to explain observations in many dynamical systems ($a_0 \approx 1.2 \times 10^{-10}\,\mathrm{m\,s^{-2}}$; Scarpa et al. 2007). Furthermore, they are thought to contain little, or no, DM – indicated by dynamical models (Phinney 1993), *N*-body simulations (Moore 1996), observations of GC tidal tails (Odenkirchen et al. 2001), dynamical and luminous masses of GCs (Mandushev, Staneva & Spasova 1991) and the lack of microlensing events from GC-mass dark haloes (Navarro, Frenk & White 1997; Ibata et al. 2002), although this is still under debate. GCs are also located at varying distances from the centre of the Galaxy, so that if all exhibit similar behaviour, Galactic influences cannot be the primary cause.

In Lane et al. (2009) (hereafter Paper I), we calculated the velocity dispersions and mass-to-light profiles of M22, M30, M53 and M68. Our conclusions were that there is no requirement for significant quantities of DM, or a modification of Newtonian gravity, to explain the kinematics of any of these clusters. In the current paper, we continue this investigation with the largest spectroscopic data set to date of 47 Tucanae (47 Tuc) and M55. We begin by describing the data acquisition/reduction (Section 2) and the membership selection for each cluster (Section 2.2). Our large samples allow us to determine a metallicity calibration based on the Tip of the Red Giant Branch (TRGB; Section 3.1), as well as the rotations (Section 3.2), systemic velocities and velocity dispersions (Section 3.3) and mass-to-light profiles (Section 3.4) – where we also place limits on the DM content of each cluster from their velocity dispersions and mass-to-light profiles. Finally, our concluding remarks are presented in Section 4.

2 DATA ACQUISITION AND REDUCTION

AAOmega, a double-beam, multi-object spectrograph on the 3.9-m Anglo-Australian Telescope (AAT) at Siding Spring Observatory in New South Wales, Australia, was employed to obtain the data for this survey. AAOmega is capable of obtaining spectra for 392 individual objects over a two degree field of view. We used the D1700 grating, which has been optimized for the Ca II infrared triplet region, centred on 8570Å, with 30 sky fibres used for optimal sky subtraction, and 5–8 fibres for guiding. The positional information for our targets was taken from the Two Micron All Sky Survey (2MASS) Point Source Catalogue (Skrutskie et al. 2006) which has an accuracy of ∼0.1 arcsec, and we selected stars that matched the $J - K$ colour and K magnitude range of the red giant branch (RGB) of each cluster.

Our observations were performed over seven nights on 2006 August 12–18, and a further eight nights on 2007 August 30 to September 6. The mean seeing was ∼1.5 arcsec. Several fibre configurations were taken for each cluster with 3600–5400 s exposures giving a signal-to-noise ratio of ∼50 − 250. To minimize scattered light cross-talk between fibres, each field configuration was limited to stars in a 3 mag range. In total, 4670 and 7462 spectra were obtained in the 47 Tuc and M55 regions, respectively. Flat field and arc lamp exposures were used to ensure accurate data reduction and wavelength calibration. The pointing accuracy of the AAT is ∼0.3 arcsec and the fibres have a ∼2 arcsec diameter. The offset due to the pointing uncertainty is azimuthally scrambled by the fibre, so has no effect on the zero-point of the wavelength calibration. Data reduction was performed with the 2DFDR pipeline,[1] which is specifically designed for AAOmega data. The efficacy of the pipeline has been checked with a comparison of individual stellar spectra.

Radial velocity and atmospheric parameters were obtained through an iterative process which takes the best χ^2 fits to synthetic spectra from the library by Munari et al. (2005) and cross-correlates this model with the observed spectra to calculate the radial velocity [a process very similar to that used by the Radial Velocity Experiment (RAVE; Steinmetz et al. 2006; Zwitter et al. 2008) project]. We used the same spectral library as the RAVE studies; Kiss et al. (2007) outline this process in detail.

2.1 Radial velocity and uncertainty estimates

To be sure that we are not under/overestimating the uncertainties, and that our radial velocity measurements, and estimates of the random uncertainties, are reproducible, we observed a single configuration of M68 (as part of the data obtained for Paper I), consisting of 317 spectra of the same stars on consecutive nights.

Radial velocities from the data for a single night were estimated using two independent pipelines to test the efficacy of our own software. For this, we compared the outputs of our own pipeline (again see Kiss et al. 2007 for a detailed description) with that from the pipeline written specifically for the RAVE project. The average difference in radial velocities between the two pipelines is $0.3 \pm 0.1\,\mathrm{km\,s^{-1}}$.

To test that our pipeline reproduces reliable velocities, and associated uncertainties, these were extracted from the data from consecutive nights. Subtracting one from the other results in a distribution with a mean of $-0.33\,\mathrm{km\,s^{-1}}$ and $\sigma \approx 0.97$. Therefore, 95 per cent of the stars observed have velocities within $\approx 2\,\mathrm{km\,s^{-1}}$ from one night to the next. This is within the systematics of the instrument (see Section 3.3) and is comparable to the quoted uncertainties for individual velocity estimates. Furthermore, because we used many fibre configurations for each cluster, it was necessary to test for systematic offsets between configurations. Therefore, we calculated the velocity dispersion of stars from four separate configurations within the same distance bin (13 stars were available from each configuration). The dispersions between configurations had a maximal difference of $0.3\,\mathrm{km\,s^{-1}}$, which is well within the uncertainties of the bin.

2.2 Cluster membership

We selected cluster members using four parameters, namely the equivalent width of the calcium triplet lines, surface gravity ($\log g$), radial velocity and metallicity ([m/H]). Only stars that matched all criteria were judged to be members. A further cut of $\log g < 3.25$ was applied to 47 Tuc to ensure as many Galactic stars were as possible were removed. This very probably removed some cluster members but was a necessary sacrifice to ensure our sample was as free of Galactic contaminants as possible. Fig. 1 shows the selection criteria of 47 Tuc. The selections of M55 are not shown because the velocity of the cluster ($\sim 175\,\mathrm{km\,s^{-1}}$) is far removed from the Galactic population ($\sim 0\,\mathrm{km\,s^{-1}}$), so the selections are very clean.

It should be noted that for several clusters studied in Paper I, a cut-off of $T_{\rm eff} \gtrsim 9000\,\mathrm{K}$ was necessary to remove hot horizontal branch (HB) stars with highly uncertain radial velocities because the calcium triplet in very hot stars is replaced by hydrogen Paschen lines (and also have intrinsic radial velocity variability, see Section 3.3). No cut was made on $T_{\rm eff}$ for either of the current clusters because no stars with $T_{\rm eff} \gtrsim 7050\,\mathrm{K}$ (for 47 Tuc) or $T_{\rm eff} \gtrsim 8500\,\mathrm{K}$ (for M55) remained after our selection process. Fig. 2 shows the

[1] http://www2.aao.gov.au/twiki/bin/view/Main/CookBook2dfdr

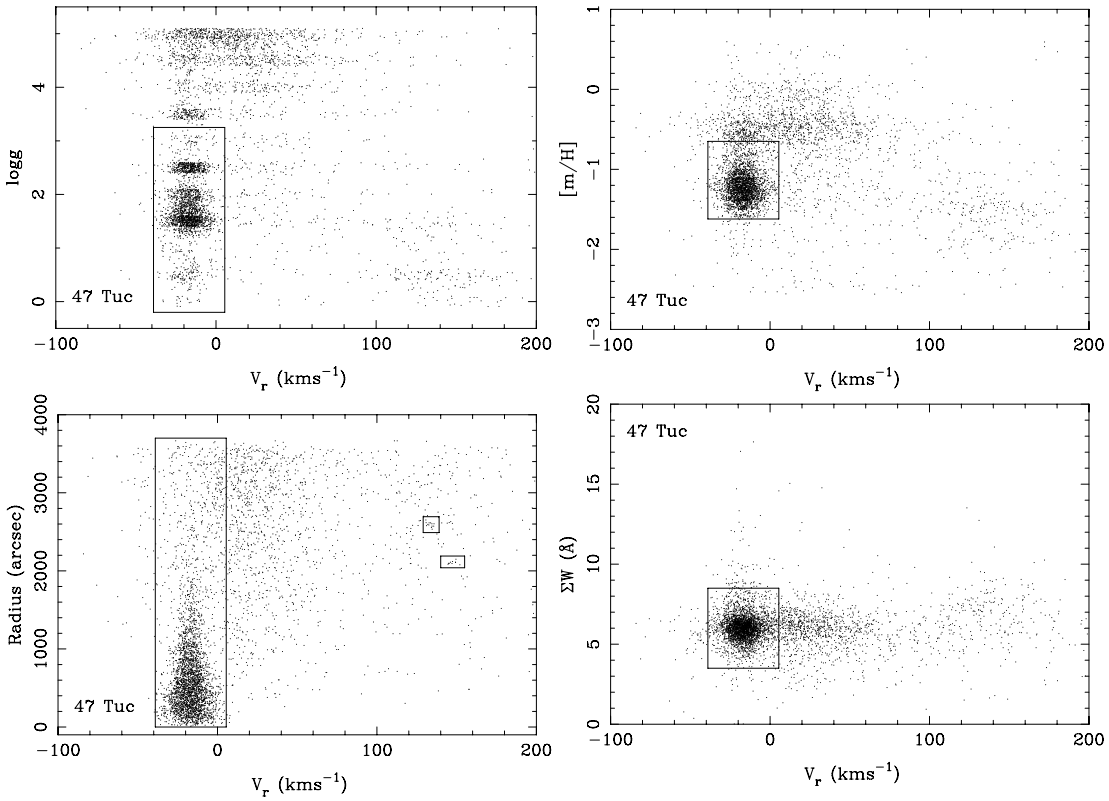

Figure 1. The selections made for 47 Tuc. The boxes indicate the selections on each parameter. The lower left panel also shows the selections for Kron 3 (at ∼2600 arcsec radius) and NGC 121 (at ∼2100 arcsec radius). The selection box for Kron 3 is centred on the cluster and was restricted to the cluster diameter (204 arcsec). For NGC 121, there were no stars outside 150 arcsec despite the diameter being similar to that of Kron 3.

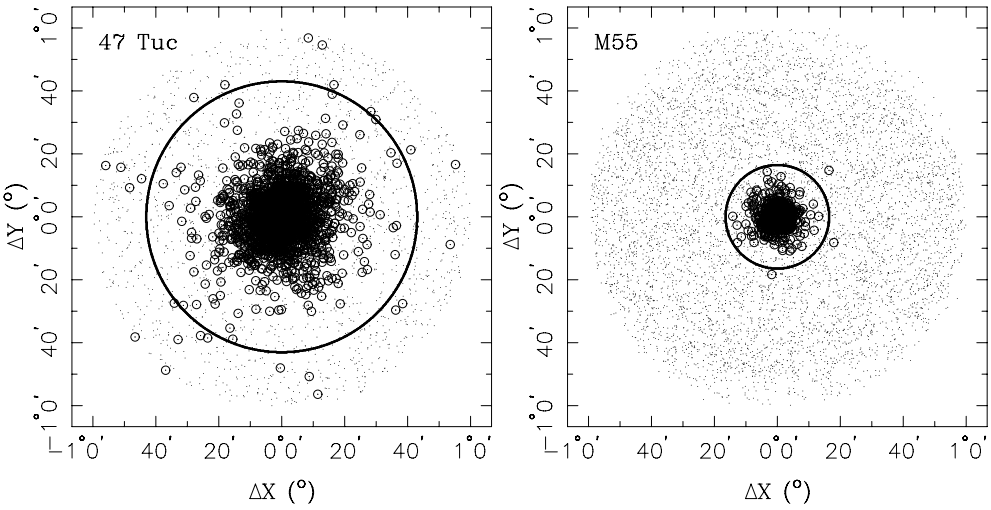

Figure 2. The uncircled points are the stars which were observed and determined not to be cluster members. The members used for analysis, based on the selection method described in the text, are circled points. The large circle is the tidal radius of the cluster from Harris (1996). In each panel, north is up and east is to the left.

relative locations of the observed stars and highlights those found to be members. Several member stars in each cluster were found beyond the tidal radius; the implications of this are discussed in Section 3.3.1.

Fig. 3 shows the colour–magnitude diagrams (CMDs) of the cluster members, with the extra-tidal stars as large points. These extra-tidal stars do not populate any specific region of the CMD, indicating that there is no systematic contributing to their selection as members. The HB, RGB bump and asymptotic giant branch (AGB) clump are all visible in 47 Tuc. A hint of the HB can be seen in M55 at $\sim 13 < J < 14$, however, it is not well populated because, unlike 47 Tuc, M55 has a blue HB, and these stars are too hot to exhibit strong calcium triplet spectra. A total of 2241 and 726 members were selected for 47 Tuc and M55, respectively. For 47 Tuc, 98.6 per cent of our final sample used for analysis (2210 out of 2241 stars) fall within the 99.7 per cent confidence level for

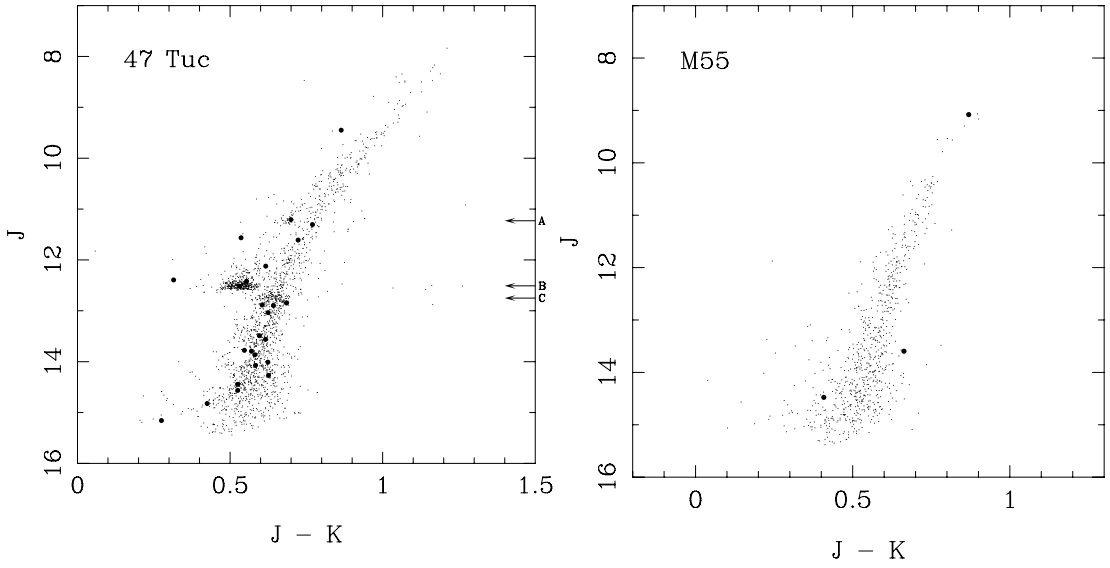

Figure 3. CMDs of selected members of 47 Tuc and M55 with extra-tidal stars shown as large points. Because these do not populate any particular part of the CMD, there is no systematic contributing to their selection as members. Note the AGB clump (A), horizontal branch (B) and RGB bump (C) in 47 Tuc. The HB of M55 at $\sim 13 < J < 14$ is sparsely populated because it has a blue HB whose stars are too hot for strong calcium triplet spectra.

cluster membership based on statistical analysis of each selection parameter.

2.2.1 Sgr, NGC 121 and Kron 3

M55 resides in front of the southern tidal tail of the Sagittarius dwarf galaxy (Sgr; Ibata, Gilmore & Irwin 1994) and 42 stars from that field were found to be part of Sgr (see Section 3.1 for details). These were removed from the sample and analysed separately. Two GCs from the Small Magellanic Cloud (SMC) are present in the 47 Tuc field, namely NGC 121 and Kron 3. When determining Kron 3 membership, we restricted our selection to a box centred on the cluster with a length of 204 arcsec, the diameter of the cluster as quoted by Bica & Dutra (2000) (Fig. 1). For NGC 121, we simply selected the clump of stars shown in Fig. 1 because there were no stars outside ∼150 arcsec, despite the diameter of this cluster being about the same as that of Kron 3 (Bica & Dutra 2000). We then overplotted the selections on the 2MASS region around 47 Tuc to ensure they fell in the same region of sky as the cluster and discarded those that did not (Fig. 4). A total of 10 and 11 stars were found to be members of NGC 121 and Kron 3, respectively.

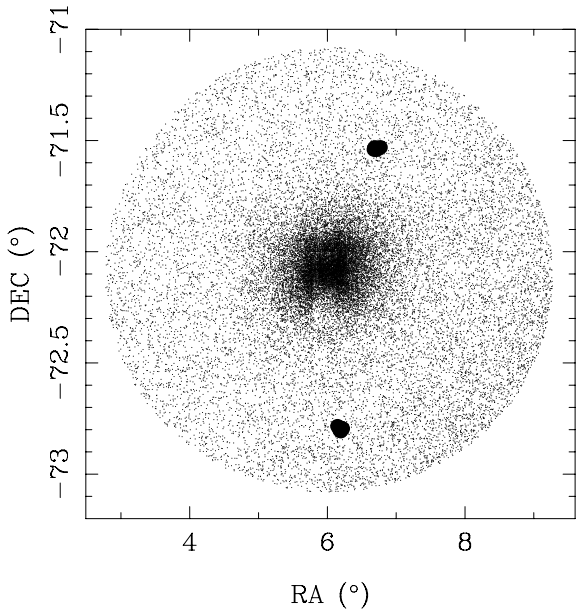

Figure 4. Selected members of Kron 3 [large points below 47 Tuc: (RA,Dec.) ≈ (6.19, −72.79)] and NGC 121 [large points above 47 Tuc: (RA,Dec.) ≈ (6.70, −71.54)].

3 RESULTS

3.1 Metallicity

Given the large sample sizes of both clusters, we were able to perform an accurate metallicity calibration in a similar way to that by Cole et al. (2004) and Warren & Cole (2009). Our method uses the TRGB K magnitude ($K_{\rm TRGB}$), instead of the HB used by Cole et al. (2004) and Warren & Cole (2009). Both methods are robust, but the TRGB is brighter than the HB, allowing our method to be used for more distant clusters where the HB is not visible. In addition, only in the K band has a direct calibration of the TRG been made with *Hipparcos* parallaxes (Tabur, Kiss & Bedding 2009). The metallicity calibration was carried out in three steps. First, $K_{\rm TRGB}$ was subtracted from each star and plotted against the equivalent width of the calcium triplet lines (see Fig. 5), giving a distance independent measure of the luminosity. $K_{\rm TRGB}$ values were taken from Valenti, Ferraro & Origlia (2004) (47 Tuc, M30 M55 and M68), Marconi et al. (1998) (Sgr core) and 2MASS CMDs (Kron 3, NGC 121, M22 and M53; see below). Several stars from the M55 field overlapped the 47 Tuc region in this figure. Because the metallicity of 47 Tuc is similar to that of the tidal tails of Sgr (e.g. Chou et al. 2007), this overlap was expected; these stars belong to the southern tidal tail of Sgr and are highlighted in Fig. 5. All stars with $T_{\rm eff} > 6000$ K were removed from the M55 sample for the metallicity analysis because these hotter HB stars have the calcium triplet lines affected by hydrogen Paschen lines and, therefore, should not be used for metallicity analysis. This was not necessary for 47 Tuc since the

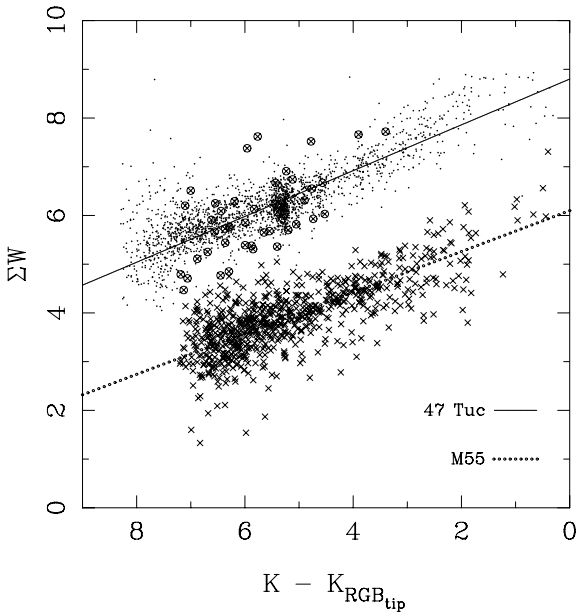

Figure 5. $K - K_{\rm TRGB}$ versus equivalent width of the calcium triplet lines. Crosses are M55 members, dots are 47 Tuc members and circled crosses are those stars determined to belong to the southern tidal tail of Sgr. These were analysed separately. The straight lines are the linear fits to the data once the Sgr members, and all stars having $T_{\rm eff} > 6000$ K, were removed.

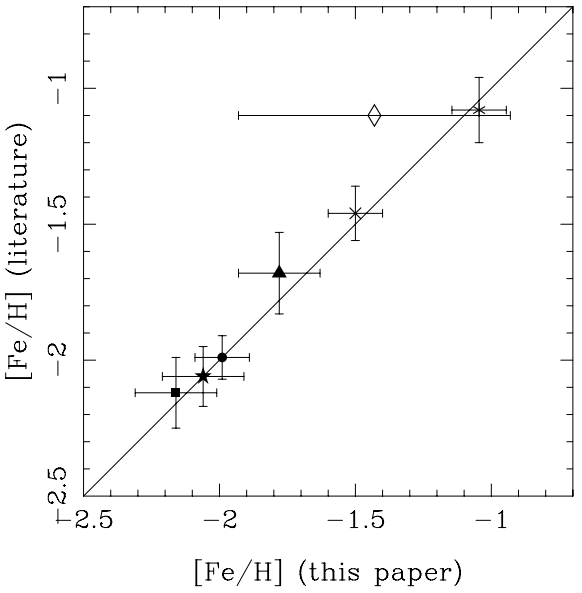

Figure 6. Calculated [Fe/H] for M30 (square), M68 (star), M53 (circle), M22 (triangle), NGC 121 (cross), Sgr (diamond), Kron 3 (asterisk) versus literature values (see text). The large uncertainty for Sgr is due to the difficulty in calculating the TRGB for this object. No consensus on an uncertainty estimate has been reached, hence none is shown here from the literature.

selections were restricted to stars with $\log g < 3.25$, because this cluster is closer to the Galaxy in $\log g$, which removed all the hotter HB stars.

The second step in the calibration process was to fit straight lines to the data (Fig. 5). Because our 47 Tuc sample contains many HB stars, and these were not expected to exhibit the same relation between calcium triplet line widths and $K - K_{\rm TRGB}$, these fits were also performed with the HB stars of 47 Tuc removed. No difference in the fits was found, so the HB stars are included in Fig. 5. The slope of these lines are 0.47 and 0.42 for 47 Tuc and M55, respectively (cf. 0.64 for V-band analysis of the HB by Cole et al. 2004 and 0.47 for K-band analysis of the HB Warren & Cole 2009).

Thirdly, by plotting [Fe/H] of the two clusters (from Harris 1996) versus $\Sigma W - AX$, where A is the gradient of the slope above and X is $K - K_{\rm TRGB}$, for these two clusters we have a calibrator on [Fe/H] (see Cole et al. 2004; Warren & Cole 2009, for a detailed discussion of this calibration methodology). $\Sigma W - AX$ can then be calculated for any cluster and therefore [Fe/H]. Fig. 6 shows [Fe/H] calculated by this method versus [Fe/H] from the literature: for Sgr (Chou et al. 2007), Kron 3 (Glatt et al. 2008b), NGC 121 (Glatt et al. 2008a) as well as the four clusters from Paper I, namely M22 (Monaco et al. 2004), M30 (Harris 1996), M53 (Harris 1996) and M68 (Harris 1996) (TRGB values for these final four clusters were all measured from 2MASS CMDs), showing this calibration for [Fe/H] to be robust. For clarity, the [Fe/H] values from this paper, and the literature, are also shown in Table 1.

The large uncertainty for Sgr is due to the difficulty in determining an accurate measure of the TRGB for this object, because the Sgr tidal tails are close to the Galaxy in colour–magnitude space (e.g. Marconi et al. 1998). Furthermore, there is a metallicity gradient along the tails. To determine the K magnitude of the TRGB for the southern Sgr tail at the location covered in the current survey, we produced a CMD from our data (Fig. 7) and found $K_{\rm TRGB} \approx 11.15$.

Table 1. [Fe/H] values from this paper and from the literature, in order of decreasing metallicity.

Cluster	[Fe/H] (this paper)	[Fe/H] (literature)
Kron 3	-1.05 ± 0.1	-1.08 ± 0.12
Sgr	-1.4 ± 0.5	~ -1.1
NGC 121	-1.5 ± 0.1	-1.46 ± 0.1
M22	-1.78 ± 0.15	-1.68 ± 0.15
M53	-1.99 ± 0.1	-1.99 ± 0.08
M68	-2.06 ± 0.15	-2.06 ± 0.11
M30	-2.16 ± 0.15	-2.13 ± 0.13

Note. The literature values are taken from Kron 3 (Glatt et al. 2008b), Sgr (Chou et al. 2007), NGC 121 (Glatt et al. 2008a), M22 (Monaco et al. 2004), M53 (Harris 1996), M68 (Harris 1996) and M30 (Harris 1996).

The paucity of stars in this CMD introduces large uncertainties into the calculated [Fe/H] for this object (Fig. 6).

Since no literature values of the $K_{\rm TRGB}$ are available for Kron 3, NGC 121, M22 or M53, we produced CMDs from 2MASS of stars within 2 arcmin of the cluster core (for M22 and M53) and within 10 arcsec for Kron 3 and NGC 121. Several hundred stars in the CMDs for M22 and M53, and ∼100 for Kron 3 and NGC 121, meant that accurate values could be calculated.

3.2 Rotation

Assuming each cluster has an isothermal distribution, their rotations were measured by halving the cluster by position angle (PA) and calculating the mean radial velocity of each half. The two mean velocities were then subtracted. This was performed in steps of 10°, and the best-fitting sine function overplotted. The results are presented in Fig. 8.

This method gives an amplitude that is twice the actual measured rotation. Therefore, 47 Tuc exhibits rotation at $2.2 \pm 0.2\,{\rm km\,s^{-1}}$

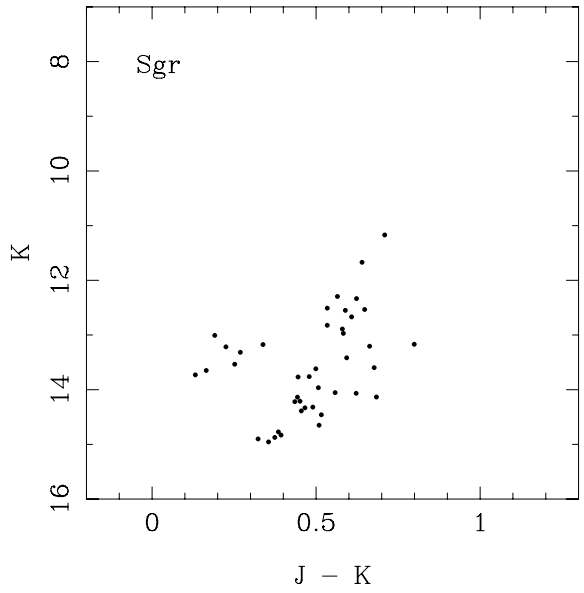

Figure 7. CMD of Sgr stars extracted from the M55 field showing the TRGB at $K \approx 11.15$.

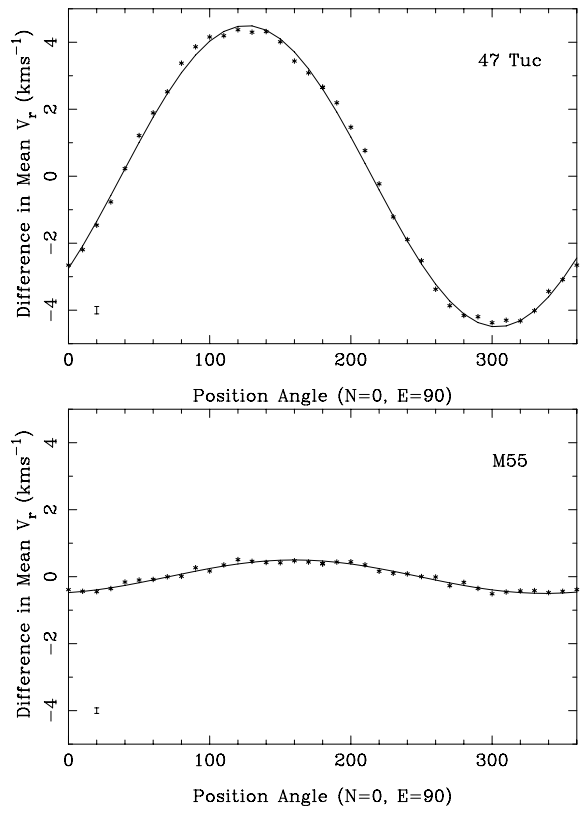

Figure 8. The rotation of each cluster calculated as the difference between the mean velocities on each side of the cluster along equal PAs, as described in the text. The best χ^2 fit sine function is overplotted, and a typical error bar is represented in the lower left of each panel.

with an approximate projected rotational axis along the line PA = 40°–220°, and M55 shows rotation at a level of 0.25 ± 0.09 km s^{-1} and an approximate axis of rotation along the line PA = 65°–245°. Our rotation measure for 47 Tuc corresponds to the value calculated by Meylan & Mayor (1986) at a radius of ≈20 pc and by Strugatskaya (1988) at ≈36 pc. Székely et al. (2007) showed that M55 is rotating with a velocity of ∼0.5 km s^{-1}. This discrepancy can probably be attributed to Székely et al. (2007) having a sample size approximately half that of the current study. For both clusters, we corrected the individual stellar velocity data for the measured rotation before the velocity dispersions, and M/L_V profiles, were calculated.

3.3 Velocity dispersions

Fig. 9 shows velocity versus *J* magnitude for the 47 Tuc data. It appears that the HB population (labelled 'B') has the greatest velocity dispersion of any stellar population in our sample. Stellar pulsations can alter the velocity dispersion profile of a GC, if pulsating stars are present in sufficient numbers, so it is important to check for this effect. 47 Tuc only has one single known RR Lyrae star (Bono et al. 2008), so this will not affect the dispersion profile; however, it is natural to expect that the large number of HB stars in this sample to have an effect, since HB stars are known to pulsate when located close to the instability strip. To test this, we calculated the velocity dispersion of the 47 Tuc sample in *J* magnitude bins. The bin containing the HB stars ($12.43 < J < 12.59$) has a velocity dispersion of 7.5 ± 0.3 and the overall dispersion is 7.5 ± 0.6. Because these stars do not show an increase in dispersion compared with the complete sample, and, furthermore, are distributed evenly throughout the cluster (Fig. 10), we see no reason to exclude the HB stars from the velocity dispersion analysis. Our M55 sample contains very few HB stars (see Fig. 3) so this effect is negligible in this cluster.

We measured the systemic velocity of each cluster, using a Markov Chain Monte Carlo (MCMC) maximum likelihood method (Gregory 2005), which takes into account the individual velocity uncertainties on the stars, providing the systemic velocity with associated uncertainties. A comparison between our values and those from the Harris (1996) catalogue are shown in Table 2. The velocities show systematic differences of the order of 2–3 km s^{-1} between our mean values and those in Harris (1996). These

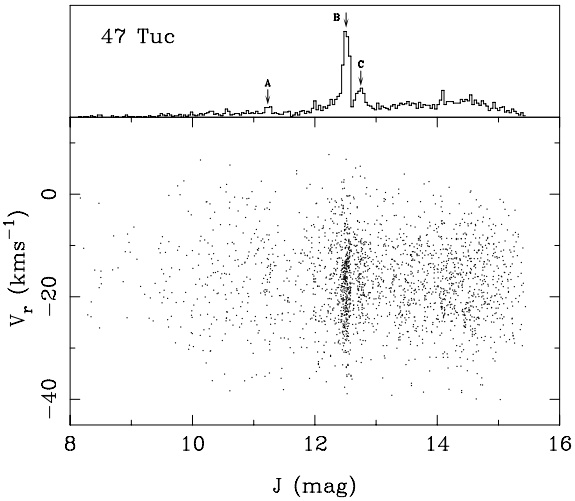

Figure 9. Velocity versus *J* magnitude of the members of 47 Tuc. The HB stars (B) appear to have the largest velocity dispersion of any stellar type. As per Fig. 3, the AGB clump is labelled 'A', the horizontal branch 'B' and the RGB bump 'C'.

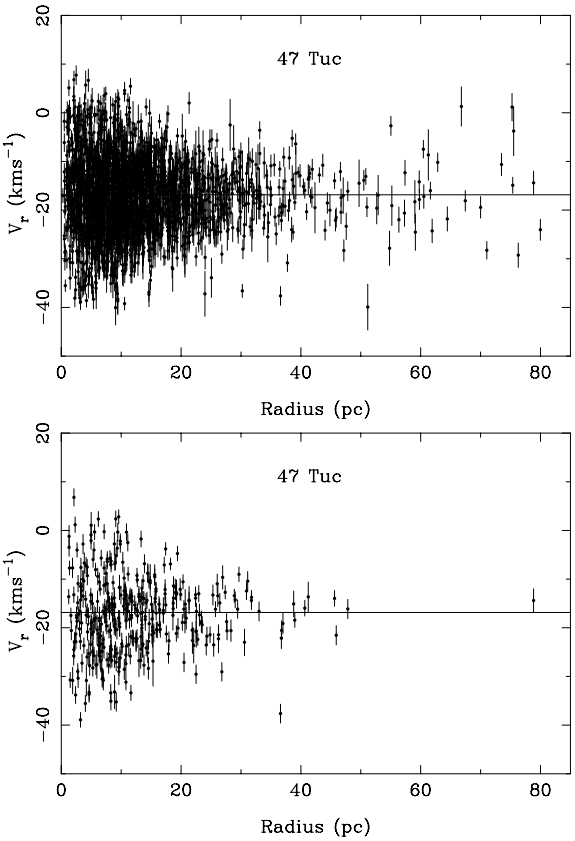

Figure 10. Velocities, and associated uncertainties, versus distance of 47 Tuc. Complete sample (top panel) and HB stars only (bottom panel). Note that the HB stars are evenly distributed throughout the cluster. The horizontal line denotes the measured systemic velocity.

Table 2. Comparisons between the systemic radial velocities of each cluster in the Harris (1996) catalogue and those from this survey.

Cluster	V_r (Harris 1996)	V_r (this paper)
47 Tuc	-18.7 ± 0.2	-16.85 ± 0.16
M55	174.8 ± 0.4	177.37 ± 0.13

Note. Velocities are in km s^{-1}.

differences are similar to what Balog et al. (2009) found for two open clusters, NGC 2451A and B, using the same instrument and analysis method and comparing data to velocities in the literature. Our interpretation is that there might be a systematic uncertainty in the zero-point of our velocity system.

To determine the velocity dispersions of our samples, we binned the stars in annuli centred on the cluster centre, ensuring approximately equal number of stars per bin (∼50 for M55 and ∼100 for 47 Tuc; see Table 3 for the bin dimensions). The MCMC method described above was then used to determine the dispersion in each bin, and the resulting velocity dispersion profiles were overplotted with the best-fitting Plummer (1911) model. The central velocity dispersion and the scale radius (r_s; containing half the cluster mass) were used for the fitting. The Plummer model allows for the calculation of the total cluster mass from the central velocity dispersion (σ_0) and r_s via (see Dejonghe 1987 for a discussion of Plummer models and their application):

$$M_{\rm tot} = \frac{64\sigma_0^2 r_{\rm s}}{3\pi G}.$$

Table 3. Dimensions of the bins, and the number of stars in each, used in the velocity dispersion analysis.

47 Tuc		M55	
Inner bin edge	Stars per bin	Inner bin edge	Stars per bin
0.000	99	0.00	51
2.131	102	1.41	45
3.048	99	1.98	49
4.031	99	2.62	52
4.834	101	3.14	49
5.698	100	3.76	51
6.416	100	4.29	45
7.210	100	4.71	55
8.080	100	5.32	47
8.894	100	6.05	50
9.699	100	6.89	49
10.600	100	7.73	52
11.460	100	8.97	49
12.409	100	11.12	44
13.347	99	15.00	38
14.713	101		
15.849	100		
17.647	100		
19.484	100		
21.899	100		
25.069	100		
30.220	100		
46.704	41		

Note. Only the inner bin edges are shown. Values given are parsecs from the centre of the cluster. The final bin extends to 80 pc for 47 Tuc and 35 pc for M55.

Twenty five extra-tidal stars were found to be members of 47 Tuc ($r_t \sim 56$ pc; Harris 1996). The velocity dispersion of 47 Tuc shows a marked increase for $R \gtrsim 28$ pc (this is discussed in Section 3.3.1). Because of this increase in velocity dispersion in the outer regions, the outer two bins were excluded from the Plummer model fitting to the dispersion profiles (Fig. 11), since including them in the fit would have created an artificial increase in the fit over the entire cluster, and hence artificially altered the total mass, scale radius and central dispersion estimates. For M55, only 3 extra-tidal stars were found to be members, and since there is no increase in the dispersion profile, these are not affecting the profile in the outskirts of the cluster. The total masses, scale radii and central velocity dispersions are presented in Table 4. Our mass estimates agree well with other studies (e.g. Meylan 1989; Pryor & Meylan 1993; Meziane & Colin 1996; Kruijssen & Mieske 2009), none of whom used Plummer models to calculate their estimates.

Scarpa et al. (2003, 2004a,b) showed an apparent flattening of the velocity dispersion profiles of five of the six GCs studied, indicating a significant DM component, or a modified theory of gravity, was required to explain their results. MOG models generally differ from Newtonian gravity for large accelerations (e.g. in galaxy clusters or elliptical galaxies) but become Newtonian for intermediate accelerations [e.g. for solar system bodies; see Moffat & Toth (2008) as an example]. MOND, however, becomes non-Newtonian for accelerations below about 1.2×10^{-10} m s^{-2} (Milgrom 1983), approximately the regime where DM is invoked to explain, for example, rotation curves of galaxies.

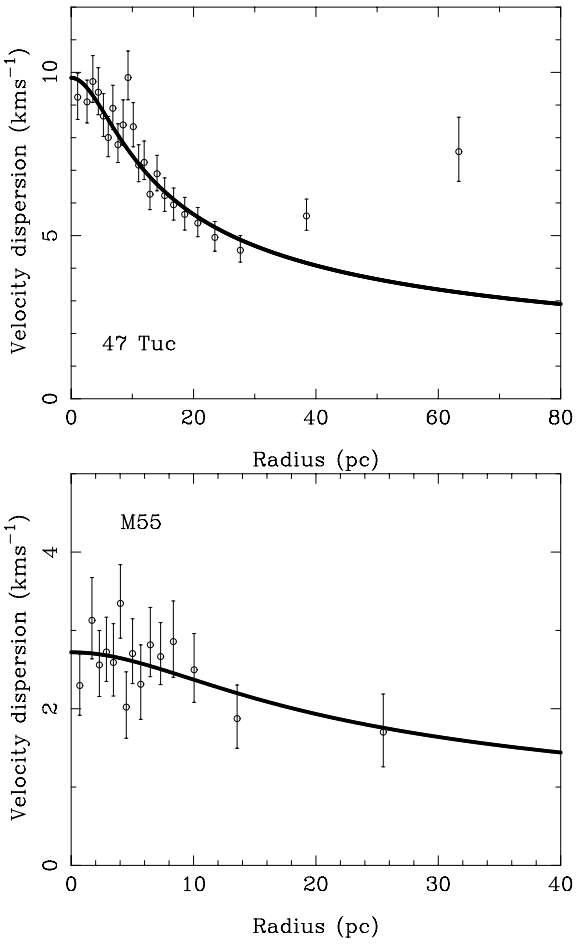

Figure 11. Velocity dispersion profiles of each cluster. The best-fitting Plummer (1911) model is overplotted. Note that for 47 Tuc the outermost two bins are not included during the fitting process to ensure no artificial increase in the estimates of total mass, r_s or central dispersion.

Table 4. Total masses, scale radii (r_s) and central velocity dispersions (σ_0) for 47 Tuc and M55.

Cluster	Total mass ($M_\odot$)	r_s (pc)	σ_0 (km s^{-1})
47 Tuc	$1.1 \pm 0.1 \times 10^6$	7.8 ± 0.9	9.6 ± 0.6
M55	$1.4 \pm 0.5 \times 10^5$	11.7 ± 4.2	2.7 ± 0.5

Plummer models have the advantage of being monotonically decreasing and, therefore, any flattening of the profiles would be discernible. Within the limits of the model, and the uncertainties in the data, neither velocity dispersion exhibits any flattening, although the profile of 47 Tuc exhibits an increase in its dispersion. This could not be called 'flattening' and a MOND/MOG model, or DM, is not required to explain this phenomenon, although a DM component may be one explanation (see Section 3.3.1). Therefore, we infer that neither DM nor a modification to the current understanding of gravitation is needed to explain the dynamics of either 47 Tuc or M55, corroborating earlier results in Paper I for M22, M30, M53 and M68, and similar conclusions by Sollima et al. (2009) for ω Centauri and Jordi et al. (2009) for Pal 14.

Because we only sampled 10 and 11 stars from NGC 121 and Kron 3, respectively, it was not possible to create a velocity dispersion *profile* for these objects. Instead, a single velocity dispersion value for the cluster was calculated, with NGC 121 having a velocity dispersion of 2.2 ± 1.1 km s^{-1} and Kron 3 of 1.8 ± 0.9 km s^{-1}.

3.3.1 Evaporation

GCs are known to be tidally destroyed by their host galaxy through tidal heating (e.g. Pal 5; Odenkirchen et al. 2003). The tidal stripping signature is evidenced by stars being stripped in two directions (the leading and trailing tidal streams). Because the sampled field around 47 Tuc does not reach far outside the tidal radius (Fig. 2), it is not possible to tell whether the extra-tidal stars exhibit a preferential direction. Therefore, an inspection of a $20^\circ \times 20^\circ$ region centred on 47 Tuc was performed, using 2MASS data selected on the RGB and HB colours/magnitudes of 47 Tuc. No evidence for extended tidal structure was observed, independently confirming the result by Leon, Meylan & Combes (2000) who found no convincing statistical evidence of tidal tails.

Evaporation in GCs has been shown to occur due to internal two-body relaxation over the cluster lifetime (e.g. McLaughlin & Fall 2008), particularly during core-collapse, or in post-core-collapsed clusters. Importantly, *N*-body simulations have shown that this evaporation exhibits a signature in the velocity dispersion profile, increasing the dispersion at $r_t/2$, precisely the region where our 47 Tuc profile increases (Drukier et al. 2007; for 47 Tuc, $r_t/2 \approx 28$ pc). Furthermore, the extra-tidal velocity distribution is symmetric about the systemic velocity (Fig. 10) implying that these stars are being accelerated in a symmetric way into the outer regions of the cluster. Drukier et al. (2007) pointed out that this evaporation is exacerbated by the collapse of a GC core, leading to greater numbers of two-body interactions. This leads to greater numbers of stars accelerated to the outer regions of the cluster, and beyond, increasing evaporation. It is this evaporation scenario that we infer for 47 Tuc, from its velocity dispersion at large radii, adding to the growing body of evidence that 47 Tuc is in a core-collapse, or post-core-collapse, phase (e.g. Gebhardt et al. 1995; Robinson et al. 1995; Howell, Guhathakurta & Gilliland 2000, and references therein).

To confirm that our interpretation is valid, and that we are not simply describing a chance phenomenon, we rebinned the data to have $\sim$50 stars per bin. The velocity dispersion profile is unaltered by the different binning. Furthermore, we changed the bin boundaries to be sure that this increasing velocity dispersion is real, and, again, found no difference in the overall shape of the profile. Of course, alternative explanations exist for the increase in dispersion. For example, if GCs form in a similar fashion to Ultra Compact Dwarf galaxies, there may be a large quantity of DM in the outskirts of the cluster as discussed by Baumgardt & Mieske (2008). However, no evidence exists supporting GCs forming in this manner. A full MCMC analysis of the outermost, apparently evaporating, stars will be performed in a subsequent paper.

3.4 Mass-to-light profiles

In dynamical systems such as elliptical and dwarf galaxies, large quantities of DM are evidenced by high mass-to-light ratios ($M/L_V \gg 1$). DM causes higher stellar accelerations, leading to inherently higher maximal stellar velocities, and hence a larger velocity dispersion. Therefore, one method for determining whether a pressure-supported object like a GC is DM dominated is to measure its M/L_V from its velocity dispersion. For our M/L_V profiles, we have used the surface brightness profiles by Trager, King & Djorgovski (1995), converted to solar luminosities per square parsec and our density profiles were calculated using (Dejonghe

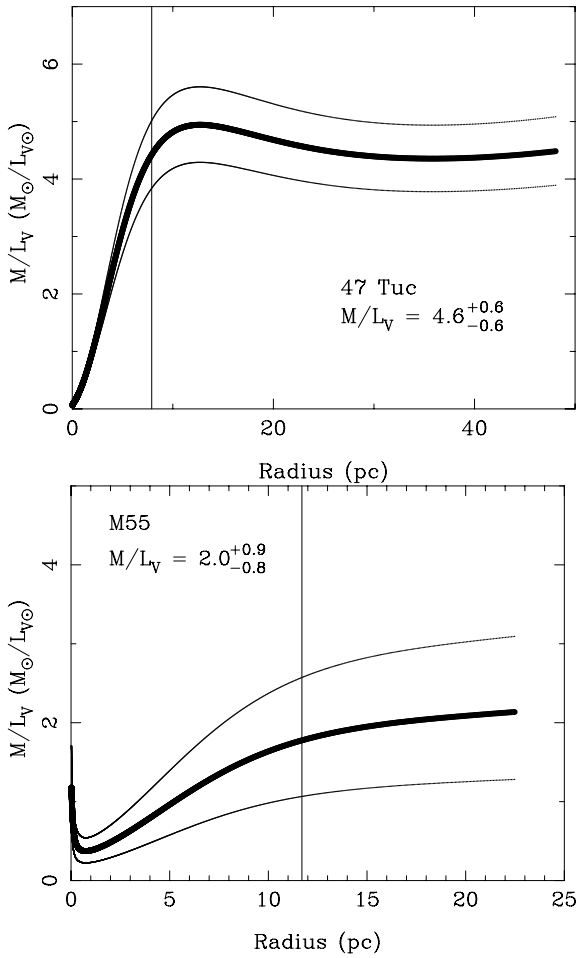

Figure 12. Mass-to-light profiles of 47 Tuc and M55. The thick line is the calculated M/L_V and the thin lines are the uncertainties. The vertical line is r_s, and the mean M/L_V is only calculated for $R > r_s$ due to the uncertainty in core mass. Neither cluster has $M/L_V \gg 1$, indicating DM is not dominant.

1987)

$$\rho(r) = \frac{M_{\rm tot}}{\pi} \frac{r_{\rm s}^2}{\left(r_{\rm s}^2 + r^2\right)^2}.$$

The M/L_V profiles, and associated M/L_V values, are shown in Fig. 12. Because of the uncertainty in core mass, the stated M/L_V values are the mean mass-to-light for $R > r_s$. Our method for calculating M/L_V is preferable to the widely adopted method using the central mass and luminosity, due to the uncertainty in core mass. Despite its apparent superiority over other methods for measuring M/L_V, very few studies have adopted it. This technique has been used by Gebhardt & Fischer (1995) for 47 Tuc, but only for the inner 10 arcmin ($\lesssim r_s$). Because the mass estimates are highly uncertain at small radii, we do not claim to have any realistic data on the M/L_V for $R < r_s$, so no comparison between the current study and that by Gebhardt & Fischer (1995) can be made.

Neither cluster has $M/L_V \gg 1$, therefore DM cannot dominate, although the larger M/L_V of 47 Tuc may indicate a small DM component. However, it has been shown that Ultra-Compact Dwarf galaxies, which follow the same luminosity – velocity dispersion relation as old GCs, show no evidence of DM for $M/L_V < 5$ (e.g. Haşegan et al. 2005; Evstigneeva et al. 2007). Because of this, we see no requirement for DM in either cluster.

4 CONCLUSIONS

Having the largest sample of spectra ever obtained for 47 Tuc and M55, we were able to produce a very accurate calibration of [Fe/H] based on the equivalent width of the calcium triplet lines and the *K*-band magnitude of the TRGB. This method is similar to that by Cole et al. (2004) and Warren & Cole (2009), except that we use the TRGB instead of the HB which means this method can be used for much more distant objects.

We calculated the rotation of our clusters assuming them to be isothermal. The rotation of 47 Tuc is $\sim 2.2 \pm 0.2$ with an approximate projected rotational axis along the line PA = 40°–220°, and M55 exhibits rotation at a level of $0.25 \pm 0.09\,{\rm km\,s^{-1}}$ and has an approximate axis of rotation along the line PA = 65°–245°. For 47 Tuc, the rotation amplitude is in good agreement with previous work (e.g. Meylan & Mayor 1986). The only previous study estimating the rotation of M55 (Székely et al. 2007) found a value about twice that of the current work, but Székely et al. (2007) had a sample size approximately half that of ours, which may explain this discrepancy.

Our calculated velocity dispersion profiles of 47 Tuc and M55 provide no evidence that either DM or a modification of current gravitational theories are required to reconcile their kinematic properties, corroborating previous work in Paper I. The dynamics of M55 are well described by a purely analytic Plummer (1911) model, which indicates that Newtonian gravity adequately describes its velocity dispersions, and shows no breakdown of Newtonian gravity at $a_0 \approx 1.2 \times 10^{-10}\,{\rm ms^{-2}}$, as has been claimed for other GCs. The internal dynamics of 47 Tuc (for $R < r_t/2$) are also very well described by the Plummer model, however, the velocity dispersion profile of 47 Tuc exhibits a large increase for $R > r_t/2$, exactly the region where evaporation due to two-body interactions in the core should be observable, especially for GCs undergoing core-collapse or in a post-core-collapse state. We interpret this increase in velocity dispersion as evaporation, and hence that this cluster is either presently in a state of core-collapse, or is a post-core-collapse GC. This adds to the growing evidence that 47 Tuc is currently undergoing a dynamical phase change (e.g. Gebhardt et al. 1995; Robinson et al. 1995; Howell et al. 2000, and references therein). A full analysis of the outer regions of this apparently evaporating cluster will be performed in a subsequent paper.

We used a Plummer model to determine the total mass, scale radius (r_s) and the M/L_V profile for each cluster. We find that neither cluster has $M/L_V \gg 1$, indicating that DM is not dominant. Within the uncertainties, our estimated cluster masses match those in the literature well, as do the M/L_V ratios (e.g. Meylan 1989; Pryor & Meylan 1993; Meziane & Colin 1996; Kruijssen & Mieske 2009). The mass-to-light profiles produced by Gebhardt & Fischer (1995) cannot be compared to the current work because they sampled the inner 10 arcmin for which the mass is uncertain. Note that we consider using mass-to-light *profiles* is a more accurate method for calculating M/L_V than using the core mass and surface brightness, because of this uncertainty.

While our results strongly indicate that the current understanding of GCs being DM poor, and their dynamics explained by standard Newtonian gravity, more robust dynamical modelling is required for confirmation.

ACKNOWLEDGMENTS

This project has been supported by the University of Sydney, the Anglo-Australian Observatory, the Australian Research Council,

the Hungarian OTKA grant K76816 and the Lendület Young Researchers Program of the Hungarian Academy of Sciences. We thank Roberto Gilmozzi for his helpful suggestions and feedback on both this paper and Paper I.

REFERENCES

Anderson J. D., Laing P. A., Lau E. L., Liu A. S., Nieto M. M., Turyshev S. G., 2002, Phys. Rev. D, 65, 082004
Angus G. W., Famaey B., Zhao H. S., 2006, MNRAS, 371, 138
Balog Z., Kiss L. L., Vinkó J., Rieke G. H., Muzerolle J., Gáspár A., Young E. T., Gorlova N., 2009, ApJ, 698, 1989
Baumgardt H., Mieske S., 2008, MNRAS, 391, 942
Bica E., Dutra C. M., 2000, AJ, 119, 1214
Bono G. et al., 2008, ApJ, 686, L87
Chou M.-Y. et al., 2007, ApJ, 670, 346
Cole A. A., Smecker-Hane T. A., Tolstoy E., Bosler T. L., Gallagher J. S., 2004, MNRAS, 347, 367
de Diego J. A., 2008, Rev. Mex. Astron. Astrofis., 34, 35
Dejonghe H., 1987, MNRAS, 224, 13
Drukier G. A., Cohn H. N., Lugger P. M., Slavin S. D., Berrington R. C., Murphy B. W., 2007, AJ, 133, 1041
Durrer R., Maartens R., 2008, preprint (arXiv:0811.4132)
Evstigneeva E. A., Gregg M. D., Drinkwater M. J., Hilker M., 2007, AJ, 133, 1722
Gebhardt K., Fischer P., 1995, AJ, 109, 209
Gebhardt K., Pryor C., Williams T. B., Hesser J. E., 1995, AJ, 110, 1699
Glatt K. et al., 2008a, AJ, 135, 1106
Glatt K. et al., 2008b, AJ, 136, 1703
Gregory P. C., 2005, Bayesian Logical Data Analysis for the Physical Sciences: A Comparative Approach with 'Mathematica' Support. Cambridge Univ. Press, Cambridge
Harris W. E., 1996, AJ, 112, 1487
Haşegan M. et al., 2005, ApJ, 627, 203
Howell J. H., Guhathakurta P., Gilliland R. L., 2000, PASP, 112, 1200
Ibata R. A., Gilmore G., Irwin M. J., 1994, Nat, 370, 194
Ibata R. A., Lewis G. F., Irwin M. J., Quinn T., 2002, MNRAS, 332, 915
Jordi K., Grebel E. K., Hilker M., Baumgardt H., Frank M., Kroupa P., Haghi H., Côtè P., Djorgovski S. G., 2009, AJ, 137, 4586
Kiss L. L., Székely P., Bedding T. R., Bakos G. Á., Lewis G. F., 2007, ApJ, 659, L129
Kruijssen J. M. D., Mieske S., 2009, A&A, 500, 785
Lane R. R., Kiss L. L., Lewis G. F., Ibata R. A., Siebert, Bedding T. R., Székely A., P., 2009, MNRAS, 400, 917
Leon S., Meylan G., Combes F., 2000, A&A, 359, 907
Marconi G., Buonanno R., Castellani M., Iannicola G., Molaro P., Pasquini L., Pulone L., 1998, A&A, 330, 453
Mandushev G., Staneva A., Spasova N., 1991, A&A, 252, 94
McLaughlin D. E., Fall S. M., 2008, ApJ, 679, 1272
Meylan G., 1989, A&A, 214, 106
Meylan G., Mayor M., 1986, A&A, 166, 122
Meziane K., Colin J., 1996, A&A, 306, 747
Milgrom M., 1983, ApJ, 270, 384
Moffat J. W., Toth V. T., 2008, ApJ, 680, 1158
Monaco L., Pancino E., Ferraro F. R., Bellazzini M., 2004, MNRAS, 349, 1278
Moore B., 1996, ApJ, 461, L13
Munari U., Sordo R., Castelli F., Zwitter T., 2005, A&A, 442, 1127
Navarro J. F., Frenk C. S., White S. D. M., 1997, ApJ, 490, 493
Odenkirchen M. et al., 2001, ApJ, 548, L165
Odenkirchen M. et al., 2003, AJ, 126, 2385
Phinney E. S., 1993, ASPC, 50, 141
Plummer H. C., 1911, MNRAS, 71, 460
Pryor C., Meylan G., 1993, in Djorgovski S. G., Meylan G., eds, ASP Conf. Ser. Vol. 50, Structure and Dynamics of Globular Clusters. Astron. Soc. Pac., San Francisco, p. 357
Robinson C., Lyne A. G., Manchester R. N., Bailes M., D'Amico N., Johnston S., 1995, MNRAS, 274, 547
Sanders R. H., Noordermeer E., 2007, MNRAS, 379, 702
Scarpa R., Marconi G., Gilmozzi R., 2003, A&A, 405, L15
Scarpa R., Marconi G., Gilmozzi R., 2004a, in Ryder S. D., Pisano D. J., Walker M. A., Freeman K. C., eds, Proc. IAU Symp. 220, Dark Matters in Galaxies. Astron. Soc. Pac., San Francisco, p. 215
Scarpa R., Marconi G., Gilmozzi R., 2004b, in Dettmar R., Klein U., Salucci P., eds, Proc. Sci. Vol. 55.1, Baryons in Dark Matter Halos. SISSA, http://pos.sissa.it
Scarpa R., Marconi G., Gilmozzi R., Carraro G., 2007, The Messenger, 128, 41
Skrutskie M. F. et al., 2006, AJ, 131, 1163
Sollima A., Bellazzini M., Smart R. L., Correnti M., Pancino E., Ferraro F. R., Romano D., 2009, MNRAS, 396, 2183
Steinmetz M. et al., 2006, AJ, 132, 1645
Strugatskaya A. A., 1988, Pis Astron. Zh., 14, 31
Székely P., Kiss L. L., Szatmáry K., Csák B., Bakos G. Á., Bedding T. R., 2007, Astron. Nachr., 328, 879
Tabur V., Kiss L. L., Bedding T. R., 2009, ApJ, 703, L72
Trager S. C., King I. R., Djorgovski S., 1995, AJ, 109, 218
Valenti E., Ferraro F. R., Origlia L., 2004, MNRAS, 354, 815
Warren S. R., Cole A. A., 2009, MNRAS, 393, 272
Zwitter T. et al., 2008, AJ, 136, 421

This paper has been typeset from a TEX/LATEX file prepared by the author.